Pulmonary Capillary Wedge Pressure Estimation Using Statistical Shape Models

Abhijit Adhikary[1], Sören J Backhaus[2,3], Andreas Schuster[4,5], Torben Lange[4,5], Alexander Schulz[4,5], Adelaide De Vecchi[1], Pablo Lamata[1]

[1]School of Biomedical Engineering and Imaging Sciences, King's College London, London, UK
[2]Department of Cardiology, Campus Kerckhoff of the Justus-Liebig-University Giessen, Kerckhoff-Clinic, Bad Nauheim, Germany.
[3]German Center for Cardiovascular Research (DZHK), Partner Site Rhine-Main, Bad Nauheim, Germany
[4]University Medical Center Göttingen, Department of Cardiology and Pneumology, Georg-August University, Göttingen, Germany
[5]German Center for Cardiovascular Research (DZHK), Partner Site Lower Saxony, Göttingen, Germany

Abstract

We evaluated the performance of statistical shape models (SSMs) derived from short-axis (SAX) cardiac magnetic resonance imaging (CMR) to estimate pulmonary capillary wedge pressure (PCWP) in a cohort of 68 cases with heart failure with preserved ejection fraction (HFpEF) and dyspnea. We obtained a 5% improvement in performance ($R^2 = 0.36$) using 3 principal component analysis (PCA) modes compared to the existing state-of-the-art non-invasive method ($R^2 = 0.31$), which uses a linear combination of left ventricular (LV) mass and left-atrial (LA) volume to estimate PCWP. We also evaluated the linear formula on our dataset and noticed that inconsistent LV mass-PCWP correlations limited predictive performance while the correlation between PCWP and LA volume calculated from 3D meshes was on par ($R^2 = 0.30$). Furthermore, manually calculated LA volume using the voxel-calculation method had the highest individual predictive performance ($R^2 = 0.33$) followed by PCA mode 1 ($R^2 = 0.32$). These findings underscore the potential of SSMs derived from CMR for non-invasive PCWP estimation in HFpEF patients, suggesting avenues for further improvement and clinical application.

1. Introduction

Pulmonary capillary wedge pressure (PCWP) is a surrogate for left-atrial (LA) pressure and left-ventricular (LV) filling pressure [1] and plays a crucial role in distinguishing between pulmonary hypertension (PH) subgroups [2]. It is traditionally measured using a Swan-Ganz [3] catheter, which is an invasive procedure with high costs and associated risks for the patients. Although PCWP can be derived from non-invasive ultrasound methods, these techniques can be unreliable [4]. To circumvent these issues, Garg et al. proposed a CMR-based formula ($\{\text{PCWP} = 6.1352 + (0.07204 \times \text{LAV}) + (0.02256 \times \text{LVM})\}$) to estimate PCWP using LA volume (LAV) and LV mass (LVM) [4]. In a cohort of 835 patients with a primary diagnosis of dyspnea, the formula achieved an R^2 of 0.31.

Statistical shape models (SSMs) find a compact representation of changes in anatomy [5]. They have shown the ability to infer mean pulmonary artery pressure, and we hypothesise that they can improve the accuracy of inferring PCWP beyond LA volume and LV mass metrics. To this end, we utilised 3D cubic-Hermite meshes [6] personalised to the SAX segmentations, enabling automated LA volume and LV mass calculation to evaluate Garg et al.'s formula and construct a SSM. A SSM from SAX cardiac imaging may better estimate PCWP in HFpEF patients, with preliminary evidence showing a 5% increase ($R^2 = 0.36$) over Garg et al.'s model ($R^2 = 0.31$).

2. Methods

We evaluated Garg et al.'s formula on a dataset (HFpEF-Stress Trial) [7] consisting of 68 real-time cardiac magnetic resonance (RT-CMR) cases of heart failure with preserved ejection fraction (HFpEF) and non-cardiac dyspnea patients. The dataset consists of two invasive catheter measurements of PCWP: i) at rest

 ISSN: 2325-887X DOI: 10.22489/CinC.2024.465

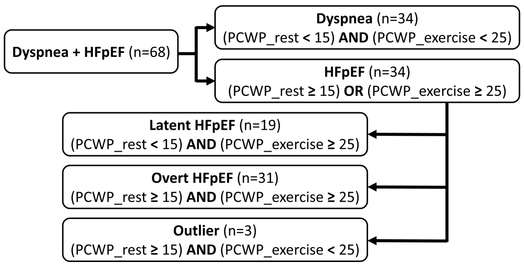

Figure 1. Distribution of aetiology in the HFpEF-Stress dataset. Blue: Left Atria, Cyan: Right Ventricle, Brown: Left Ventricular Myocardium.

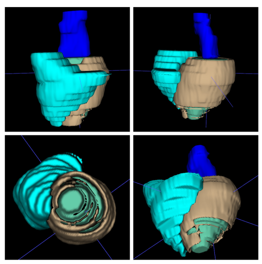

Figure 2. Exemplary SAX segmentation in our dataset.

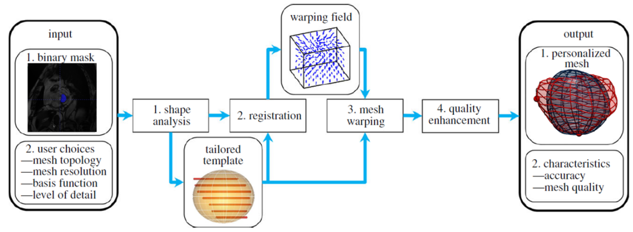

Figure 3. Mesh generation pipeline (Adapted from [9]).

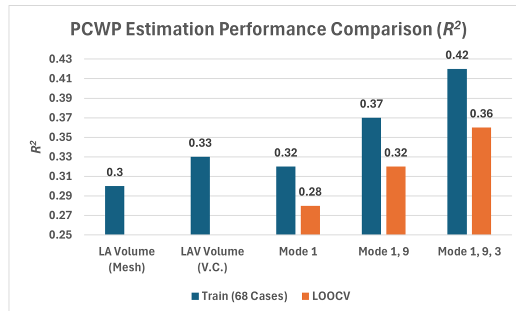

Figure 4. Performance (R^2) of PCA modes to predict PCWP with a growing number of modes aggregated. (V.C.: Voxel Calculation Method)

{PCWP$_{rest}$ ($11.16\ mmHg \pm 4.86\ mmHg$)} and ii) during exercise {PCWP$_{exercise}$ ($22.59\ mmHg \pm 8.95\ mmHg$)} and imaging sequences includes: i) SAX (see figure 2), ii) two-chamber ($2_{chamber}$) and iii) four-chamber ($4_{chamber}$) long-axis (LAX) of both the left atria (LA) and left ventricle (LV). Segmentations of the LA and LV were performed in three cardiac phases: i) End-diastole (ED), ii) Mid-diastole (MD) and iii) End-Systole (ES). Also, based on the PCWP$_{rest}$ and PCWP$_{exercise}$, we categorized our cases into subgroups (see Figure 1).

We generated cubic-Hermite meshes [6] of the LA and LV from SAX segmentations and used them to construct an LA and an LV SSM. We then extracted LAV ($97.86\ mL \pm 30.14\ mL$), LA Sphericity ($82.16\ \% \pm 3.13\ \%$) and LVM ($148.98\ g \pm 45.36\ g$) from the meshes. Using the SSM modes, we assessed their correlation with PCWP. Additionally, to enhance generalization, we employed penalized linear regression with leave-one-out cross-validation (LOOCV) [8] and gradually aggregated modes to determine the most influential combination.

2.1. Building Statistical Shape Models

Our mesh generation process involved registering a precomputed 3D template onto organ segmentation, utilizing a warping function to deform the initial template to match individual anatomy [9]. Additionally, an initial alignment process was performed requiring three vector directions: i) perpendicular to the SAX plane, ii) towards the left ventricular outflow tract, and iii) their cross-product. Subsequently, SSMs were constructed by applying Principal Component Analysis (PCA) to the meshes' degrees of freedom, projecting them into a lower-dimensional space while maximizing variance along each axis [10].

2.2. Gradual Aggregation of PCA Modes

We utilized penalized linear regression to enhance model generalization by limiting coefficient growth [8]. Our aim was to estimate PCWP accurately with minimal PCA modes while ensuring robust generalization.

We adopted a gradual aggregation strategy, initially incorporating the most individually predictive mode and progressively adding modes based on their combined predictive power. We also explored a reverse approach, initially including all modes and selectively removing those with minimal impact. The goal was to identify a converging set of consensus modes with the highest correlation with PCWP. Finally, we employed leave-one-out cross-validation (LOOCV) to maximize data utilization and generalizability within our small cohort.

2.3. Interpretation of PCA modes

We analyzed the correlation between various PCA modes and LAV and LA sphericity, along with qualitatively interpreting individual and aggregated modes by visual inspection of their 3D shapes.

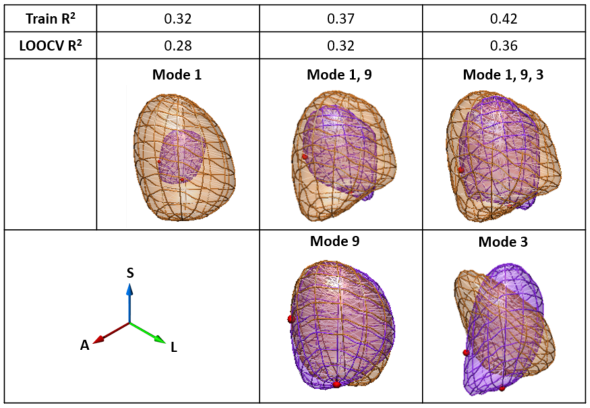

Figure 5. Illustration of the 3D models of the individual and aggregated PCA modes of the LA. The gold and purple shapes represent the two extremes explained by the modes. The two red spheres overlaid represent directions, from the centre of mass, towards the inferior direction of the SAX stack and towards the left ventricular outflow tract. (S: Superior, A: Anterior, L: Left of Atria)

3. Results

3.1. Evaluation of Garg et al.'s Formula

We evaluated Garg et al.'s formula on the HFpEF-Stress dataset using LAV and LVM mass extracted from the 3D meshes, achieving an R^2 of 0.21 compared to Garg et al.'s baseline R^2 of 0.31. To understand the 10% performance drop, we conducted individual correlation analyses of LAV and LVM with PCWP. We observed that the LA volume correlation ($R^2 = 0.30$) remained consistent with Garg et al.'s ' findings. However, LV mass correlation became insignificant ($R^2 = 0.00$) compared to Garg et al.'s ($R^2 = 0.08$), resulting in an overall decline in performance.

Furthermore, to assess the robustness of LAV and LVM extracted from meshes, we calculated LAV and LVM from the SAX segmentations using the voxel-calculation method and achieved a higher R^2 of 0.27 using the formula, attributed to a 3% increase in LAV ($R^2 = 0.33$) and a 1% increase in LVM ($R^2 = 0.01$).

Finally, to understand the insignificant correlation between LVM and PCWP, we examined its distribution across our dataset. We found that our dataset exhibited a higher mean LVM (148.98 ± 45.03) compared to Garg et al.'s dataset (96.6 ± 32.1).

3.2. PCA modes to predict PCWP and their interpretation

To explore shape patterns correlating with PCWP, we constructed SSMs from 3D meshes. We only report the results LA SSM, as the LV SSM had insignificant predictive performance. Using individual correlation analysis of the PCA modes with PCWP, we found that mode 1 had the highest correlation ($R^2 = 0.32$), followed by modes 6, 3 and 9 ($R^2 = 0.10$, $R^2 = 0.05$, $R^2 = 0.03$ respectively).

LA mode 1 is highly correlated with volume ($R^2 = 0.85$) while only 6% of the variance is explained by sphericity [11]. Furthermore, by visualizing figure 5 we notice that two extremes of PCA mode 1 explains volume. We also notice that one of the extremes (yellow) when combining modes 1, 9 and 3 resembles the LA roof-dilation towards the right pulmonary veins, while the mitral annulus elongates towards the RV apex.

3.3. Gradual aggregation of PCA modes to predict PCWP

We then performed gradual aggregation of modes using LOOCV and found that mode 1 has a cross-validation $R^2 = 0.28$, combining modes 1 and 9 results in $R^2 = 0.32$ and combining modes 1, 9 and 3 results in $R^2 = 0.36$. However, further aggregation of modes did improve LOOCV performance. The reverse approach, with gradual removal, reached the same optimal combination of modes.

4. Discussion

Our results suggest that PCWP can be reliably inferred from LA volume but not from LV mass and that the 3D morphology of the LA, as captured by an SSM, improves the ability to infer PCWP over current state-of-the-art ($R^2 = 0.36$ vs. $R^2 = 0.31$).

The ability to predict PCWP from simple metrics [4] was reproduced in our work, in agreement with recent reports [12], but with an important novel insight: LV mass was not correlated with PCWP. Consequently, an overall decrease in PCWP estimation accuracy was reported when utilizing Garg et al.'s formula (0.31 vs. 0.21). This finding may be because our population displayed a much more enlarged LV. We thus interpret that LVs with a larger mass, a sign of a later stage of remodelling, have lost the ability to further remodel with changes in PCWP.

LA volume is a stronger predictor of PCWP than LV mass, as already described [4], and our results show that manual calculation of LAV using SAX voxel-calculation demonstrated the highest individual correlation to PCWP. We expected that the personalization of 3D meshes would improve the accuracy of LAV computation and, as such, the correlation with PCWP, as demonstrated when working with LV [13] and justified by the removal of segmentation noise and artefacts achieved. Nevertheless, both volume computation from mesh and PCA mode 1, which mainly explains volume change, reported weaker performance.

In our study, we computed LA volume from a SAX, which we expected to be more accurate than the more conventional long axis acquisitions with either a single plane [14] or the bi-plane rule [4] that have been used to estimate PCWP and bi-plane volume is more accurate than a single plane [12]. Our future plan is to quantify the impact of using SAX vs. a long-axis baseline performance.

Prediction of PCWP is not only driven by LAV but also by its 3D morphology. The gradual aggregating modes report that modes with weaker individual correlations (e.g., mode 9) could significantly enhance overall performance, indicating their potential complementarity. The 3D visual inspection of the aggregated modes suggests the presence of forces that pull the right pulmonary artery upwards, mirrored by forces that pull the mitral valve region downwards. Further research is needed to validate these findings' generality and relevance.

4.1. Limitations

Despite our thorough analysis, this study has limitations. The small sample size (68 cases) may restrict generalizability, especially as we focused on HFpEF and non-cardiac dyspnea patients. Additionally, important factors like comorbidities and medication usage were not considered, potentially affecting our predictive models. Future research should include larger, more diverse cohorts to validate non-invasive PCWP estimation methods.

5. Conclusion

A SSM built from SAX cardiac imaging may better estimate PCWP in HFpEF patients, with preliminary evidence showing a 5% increase ($R^2 = 0.36$) over Garg et al.'s model ($R^2 = 0.31$).

References

[1] de Oliveira RK, Ferreira EV, Ramos RP, Messina CM, Kapins CE, Silva CM, Ota-Arakaki JS. Usefulness of Pulmonary Capillary Wedge Pressure as a Correlate of Left Ventricular Filling Pressures in Pulmonary Arterial Hypertension. The Journal of Heart and Lung Transplantation 2014;33(2):157–162.

[2] Simonneau G, Montani D, Celermajer DS, Denton CP, Gatzoulis MA, Krowka M, Williams PG, Souza R. Haemodynamic Definitions and Updated Clinical Classification of Pulmonary Hypertension. European Respiratory Journal 2019;53(1).

[3] Swan HJC, Ganz W, Forrester J, Marcus H, Diamond G, Chonette D. Catheterization of the Heart in Man with Use of a Flow-directed Balloon-tipped Catheter. New England Journal of Medicine 1970;283(9):447–451.

[4] Garg P, Gosling R, Swoboda P, Jones R, Rothman A, Wild JM, Kiely DG, Condliffe R, Alabed S, Swift AJ. Cardiac Magnetic Resonance Identifies Raised Left Ventricular Filling Pressure: Prognostic Implications. European Heart Journal 2022;43(26):2511–2522.

[5] Varela M, Bisbal F, Zacur E, Berruezo A, Aslanidi OV, Mont L, Lamata P. Novel Computational Analysis of Left Atrial Anatomy Improves Prediction of Atrial Fibrillation Recurrence after Ablation. Frontiers in Physiology 2017;8. ISSN 1664-042X.

[6] Lamata P, Niederer S, Nordsletten D, Barber DC, Roy I, Hose DR, Smith N. An Accurate, Fast and Robust Method to Generate Patient-Specific Cubic Hermite Meshes. Medical Image Analysis 2011;15(6):801–813.

[7] Backhaus SJ, Lange T, George EF, Hellenkamp K, Gertz RJ, Billing M, Wachter R, Steinmetz M, Kutty S, Raaz U, et al. Exercise Stress Real-time Cardiac Magnetic Resonance Imaging for Noninvasive Characterization of Heart Failure with Preserved Ejection Fraction: The Hfpef-stress Trial. Circulation 2021;143(15):1484–1498.

[8] Bousquet O, Elisseeff A. Stability and Generalization. The Journal of Machine Learning Research 2002;2:499–526.

[9] Lamata P, Sinclair M, Kerfoot E, Lee A, Crozier A, Blazevic B, Land S, Lewandowski AJ, Barber D, Niederer S, et al. An Automatic Service for the Personalization of Ventricular Cardiac Meshes. Journal of The Royal Society Interface 2014;11(91):20131023.

[10] Abdi H, Williams LJ. Principal Component Analysis. Wiley Interdisciplinary Reviews Computational Statistics 2010;2(4):433–459.

[11] Bisbal F, Guiu E, Calvo N, Marin D, Berruezo A, Arbelo E, Ortiz-Pérez J, De Caralt TM, Tolosana JM, Borràs R, et al. Left Atrial Sphericity: A New Method to Assess Atrial Remodeling. Impact on the Outcome of Atrial Fibrillation Ablation. Journal of Cardiovascular Electrophysiology 2013; 24(7):752–759.

[12] Backhaus SJ, Schulz A, Lange T, Evertz R, Kowallick JT, Hasenfuß G, Schuster A. Rest and Exercise-stress Estimated Pulmonary Capillary Wedge Pressure Using Real-time Free-breathing Cardiovascular Magnetic Resonance Imaging. Journal of Cardiovascular Magnetic Resonance 2024;26(1):101032. ISSN 1097-6647.

[13] Acero JC, Schuster A, Zacur E, Lange T, Stiermaier T, Backhaus SJ, Thiele H, Bueno-Orovio A, Lamata P, Eitel I, Grau V. Understanding and Improving Risk Assessment After Myocardial Infarction Using Automated Left Ventricular Shape Analysis. JACC Cardiovascular Imaging 2022; 15(9):1563–1574.

[14] Grafton-Clarke C, Matthews G, Gosling R, Swoboda P, Rothman A, Wild JM, Kiely DG, Condliffe R, Alabed S, Swift AJ, Garg P. The Left Atrial Area Derived Cardiovascular Magnetic Resonance Left Ventricular Filling Pressure Equation Shows Superiority over Integrated Echocardiography. Medicina 2023;59(11). ISSN 1648-9144.

Address for correspondence:

Abhijit Adhikary
School of Biomedical Engineering and Imaging Sciences, King's College London, St Thomas' Hospital, London, SE1 7EH, United Kingdom.
Abhijit.Adhikary@kcl.ac.uk